ACS PRF 57661-ND7

Rational Design and Synthesis of Well-defined Organic Linear and Janus-type Molecular Bottlebrush Cocoons as well as Star-like Molecular Bottlebrush Trilobes

Zhiqun Lin, Georgia Institute of Technology, Atlanta, GA 30332

Research Progress Report (09/01/2018-08/31/2019)

The PI proposes to synthesize well-defined organic linear and Janus-type molecular bottlebrush cocoons as well as star-like molecular bottlebrush trilobes. Linear bottlebrush cocoons and star-like bottlebrush trilobes were synthesized. They were employed as nanoreactors for the synthesis of perovskite nanocrystals (NCs) with enhanced stability. Moreover, the cocoons were applied as nanocarrier for drug encapsulation and controlled delivery.

1. Star-like Bottlebrush Trilobes

Figure 1a depicts the synthesis of star-like bottlebrush trilobes. First, star-like bottlebrush trilobes PHEMA-*g*-(PAA-*b*-*c*PS) was synthesized by sequential atom transfer radical polymerization (ATRP) of 2-hydroxyethylmethacrylate (HEMA), *tert*-butyl acrylate (*t*BA), styrene (St)/divinylbenzene (DVB, as cross-linker, 5%), followed by hydrolysis of the intermediate P*t*BA blocks into PAA. Subsequently, as-prepared star-like bottlebrush trilobes were then used as nanoreactor to produce perovskite, specifically $CsPbBr_3$, NCs with crosslinked PS (*c*PS) permanently tethered on the surface (**Figure 1b**). The precursors (CsBr and $PbBr_2$) was selectively loaded into the inner compartment of the trilobe due to strong coordination between -COOH groups of PAA and metal ions of precursors. As toluene is a good solvent for PS yet poor solvent for $CsPbBr_3$, $CsPbBr_3$ NCs were instantly form when precursor-loaded nanoreator solution was dropped into toluene. However, the flexible PHEMA backbone as well as PAA brushes on each lobe were quickly collapsed and reconfigured into spherical shape due to their poor solubility in toluene, leading to the formation of spherical $CsPbBr_3$ NCs (**Figure 2a**). The $CsPbBr_3$ NCs display a major absorption peak at 510 nm and a strong emission peak at 519 nm (**Figure 2b**).

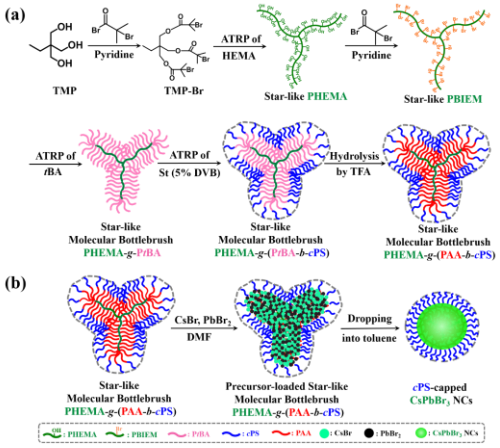

Figure 1. (a) Synthetic route to star-like molecular bottlebrush trilobe PHEMA-*g*-(P*t*BA-*b*-*c*PS). (b) *In-situ* synthesis of *c*PS-capped $CsPbBr_3$ NC using star-like PHEMA-*g*-(PAA-*b*-*c*PS) as nanoreactor.

The stabilities of *c*PS-capped $CsPbBr_3$ NCs against UV irradiation, oxygen and moisture, heat, and water were scrutinized in comparison of the OA/OAm co-capped $CsPbBr_3$ NCs synthesized by conventional method. The UV stability (**Figure 2c**), ambient stability (**Figure 2d**), thermal stability (**Figure 22**), and water stability (**Figure 2f**) tests clearly showed a negligible PL change for *c*PS-capped $CsPbBr_3$ NCs while the PL intensity of OA/OAm co-capped $CsPbBr_3$ NCs decreased dramatically when exposed to UV, water and heat. This is because OA and OAm are attached to the surface via a non-covalent coordination, which are easily detached at elevated temperature and UV-induced photo-oxidation, leading to the aggregation of NCs. *c*PS on the other hand is covalently bonded to the surface, providing a superior colloidal stability under harsh conditions. The moisture and water stabilities of *c*PS-capped $CsPbBr_3$ NCs are due to the hydrophobicity of PS that acts an effective barrier against water penetration. Likewise, the detachment of OA/OAm upon addition of water due to weak binding between OA/OAm and $CsPbBr_3$ NCs triggered a rapid degradation of $CsPbBr_3$ NCs. In contrast, *c*PS-capped $CsPbBr_3$ NCs manifested a highly improved stability in various polar organic solvents (e.g., MeOH, IPA, DMF).

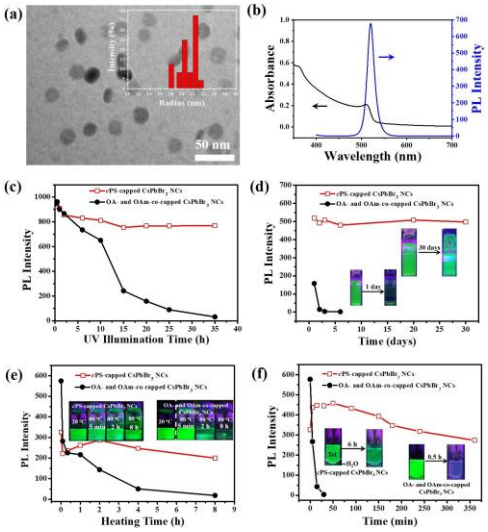

Figure 2. (a) TEM image (b) Absorption and PL spectra, (c) UV, (d) ambient, (e) thermal, (f) water stabilities of *c*PS-capped $CsPbBr_3$ NCs.

As *c*PS-capped $CsPbBr_3$ NCs display impressive stability in polar organic solvents as discussed above, they can be exploited as a probe to detect a trace amount of Cl^-/I^- (~μM) in organic solvents motivated by the facile anion exchange reaction and the associated emission tunability. The PL peak positions of *c*PS-capped $CsPbX_3$ NCs varied from 519 nm to 458 nm and to 670 nm by manipulating the amount of Cl^- and I^- added, respectively, with obvious color changes (**Figure 3a**). They correlate linearly with the anion concentrations (**Figure 3b-3c**), signifying that *c*PS-capped $CsPbBr_3$ NCs can be employed as a promising probe for Cl^- and I^- detection in organic solvents while inert to other common anions.

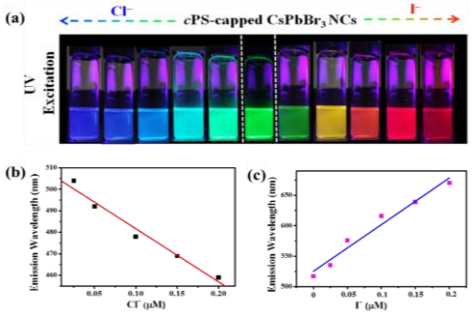

Figure 3. Digital images of *c*PS-capped $CsPbBr_3$ NCs toluene solutions upon the addition of Cl^- and I^- MeOH solutions of different amounts. The PL peak positions plotted as a function of the concentration of (b) Cl^- and (c) I^-.

2. Linear Bottlebrush Cocoons

Figure 4a shows the synthetic route to bottlebrush cocoons. Briefly, bottlebrush cellulose-*g*-(P*t*BA-*b*-P(HEMA-N_3)) was synthesized by sequential ATRP of *t*BA and HEMA from brominated cellulose, followed by two-step functionalization of the -OH groups on PHEMA into -N_3 groups. The N_3 group can be readily crosslinked by UV irradiation. The cocoons were then used as nanoreactor for synthesis of $CsPbBr_3$ nanorods (NRs) in the same manner as the trilobes noted above. The influence of surface capping polymer on the water and IV stabilities of $CsPbBr_3$ NRs were investigated. It can be clearly seen from **Figure 4b** that OA/OAm co-capped $CsPbBr_3$ NRs synthesized from conventional method has extremely poor stability that has been elaborated in the trilobe section. An increase in both water and UV stability was observed after the surface PHEMA block was crosslinked, creating a much denser surface barrier. On the other hand, when the PHEMA outer block was changed to more hydrophobic PS block, there was a significant improvement in the water stability due to heavily collapsed PS shell when getting in contact with water. However, the UV stability remained the same with uncrosslinked PHEMA-capped $CsPbBr_3$ NRs, demonstrating that surface polymer polarity only affects water stability, not UV stability of $CsPbBr_3$ NRs. Additionally, bottlebrush cocoons can also serve as effective nanocarriers for drug delivery. As shown in **Figure 4c**, the total encapsulation amount as well as the release time was extended three-fold after surface crosslinking. Meanwhile, the modulated release rate was achieved with the cocoons as the nanocarrier. Notably, the inner P*t*BA can be substituted with other functional polymers that possess special interaction with drugs or peptides to achieve selective encapsulation for targeted drug delivery.

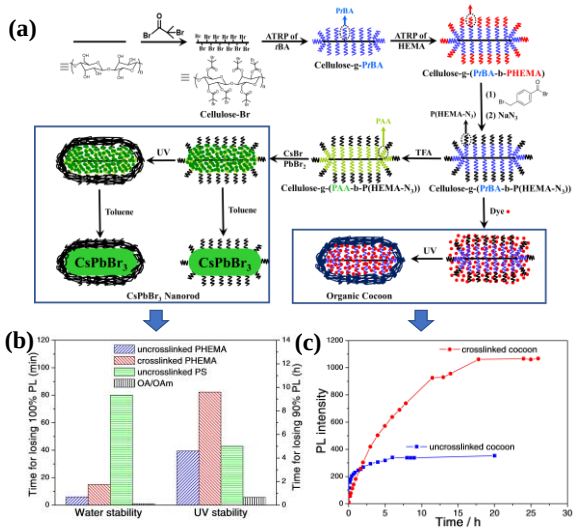

Figure 4. (a) Synthetic scheme for linear bottlebrush cocoons and $CsPbBr_3$ NRs. (b) Colloidal stability of $CsPbBr_3$ NRs. (c) Dye release profile of fluorescein-loaded cocoons.

We note that synthesis of Janus-type bottlebrush cocoons will be the focus of our future research.

Research Impact

This project renders the PI to build a new research direction in constructing polymers and block copolymers with complex architectures that are amenable to well-established living polymerization techniques. A new synthetic strategy towards highly stable perovskite NCs via a nanoreactor approach has been explored, which holds significant advantages over conventional approach. Two different surface crosslinking routes were also employed in constructing trilobe and cocoon architectures. The research project involves a set of polymer synthesis and a variety of characterization techniques. Two graduate students have been working on this project. The students working on the project have gained extensive knowledge on polymer architecture design and inorganic NC synthesis. This project also provided good opportunity for students to learn a suite of polymer characterization techniques, including GPC for measuring MW, NMR for evaluating chemical composition, AFM and TEM for examining morphology.